Swansea University
Prifysgol Abertawe

Cronfa
Setting Research Free

**Cronfa - Swansea University Open Access Repository**

This is an author produced version of a paper published in :
*Structural and Multidisciplinary Optimization*

Cronfa URL for this paper:
http://cronfa.swan.ac.uk/Record/cronfa31622

**Paper:**
Thompson, J., Walton, S., Hassan, O., Rolland, S. & Sienz, J. (2017). The use of CFD and multi-objective optimisation techniques to customise an industrial pre-mixer. *Structural and Multidisciplinary Optimization*
http://dx.doi.org/10.1007/s00158-016-1643-7

This article is brought to you by Swansea University. Any person downloading material is agreeing to abide by the terms of the repository licence. Authors are personally responsible for adhering to publisher restrictions or conditions. When uploading content they are required to comply with their publisher agreement and the SHERPA RoMEO database to judge whether or not it is copyright safe to add this version of the paper to this repository.
http://www.swansea.ac.uk/iss/researchsupport/cronfa-support/

**Structural and Multidisciplinary Optimization manuscript No.**
(will be inserted by the editor)

# The use of CFD and multi-objective optimisation techniques to customise an industrial pre-mixer

**JS. Thompson · S. Walton · O. Hassan · SA. Rolland · J. Sienz**

Received: May 2016 / Accepted: date

**Abstract** Considering the use of commercial-off-the-shelf (COTS) devices in industry, a case study has been undertaken implementing the goal driven optimisation of a venturi-type pre-mixer. This COTS device is used to supply the correct ratio of a specific fuel and oxidiser to a pre-mix burner. Providing the correct quantity of excess air results in a reduction of the $NO_x$ emissions; and this, in addition to the requirement for complete mixing of the constituents has been used to define the multi-objective optimisation of the device. A Computational Fluid Dynamics (CFD) simulation has been carried out using Fluent v14.5; verified by experimental data. To find an optimised design of the pre-mixer, four geometrical dimensions of its current design have been considered. An assessment of varying sampling and interpolation techniques has been made, in order to establish the most appropriate for use with this specific problem. The evolutionary-based NSGA-II and deterministic Nelder Mead optimisation algorithms have been used and their results compared to verify the optimisation outcome. Based on these findings, suggested customisation of the COTS pre-mixer's design could result in improvements in mixing performance, in the region of 30%.

**Keywords** pre-mixer · Fluent · multi-objective · optimisation

JS. Thompson
College of Engineering, Swansea University, Bay Campus, Swansea, SA1 8QQ
Tel.: +44-1792-602327
E-mail: jennifer.thompson@swansea.ac.uk

S. Walton
College of Science, Swansea University, Singleton Park, Swansea, SA2 8PP

# 1 Introduction

## 1.1 Motivation

Many small/medium-sized enterprises (SMEs) lack the sufficient expertise or funds to undertake the design of all components from first principles or "scratch", and instead must resort to utilising "commercial-off-the-shelf" (COTS) devices. Considering this problem, a specific, industrially focussed case study has been undertaken, which attempts to assess the suitability of a COTS pre-mixer for use with a specific burner and fuel source. The burner formed the radiative source in a heat exchanger, used in a "pressure let-down station line heater", to maintain the temperature of piped natural gas above 0 °C at gas pressure reducing stations. The pre-mixer must achieve certain mixing requirements must be achieved to ensure a satisfactorily clean burn. Multi-objective optimisation has been used to assess, what, if any gains in performance can be made. With regards the optimisation procedure, on identification of the most appropriate sampling and interpolation/meta-modelling approaches, two different optimisation algorithms have been implemented for verification purposes: an evolutionary-based Genetic Algorithm (GA); and, the deterministic Nelder Mead. Prior to any optimisation, a robust Computational Fluid Dynamics (CFD) model of the pre-mixer had to be implemented and validated.

## 1.2 Pre-mixers

Industrial burners which utilise a gaseous fuel supply are classified according to how the fuel and oxidiser are mixed; in Pre-mix Burners, as implied by the name, all of the oxidiser required for combustion is inspirated and completely mixed prior to initiation of combustion [1]. For this category of burner, increasing the excess air (oxidiser) results in a leaner mix that subsequently lowers the resulting flame temperature and reduces levels of Nitrogen Oxides ($NO_x$) emissions [2]. The minimisation of such pollutants is a highly desirable outcome, due to the health risks they pose and their environmental impact; with legislation in place for industry to reduce the production of such harmful emissions [3]. Consequently, especially low emissions are a highly marketable aspect of commercial combustion systems.

The oxidiser and gaseous fuel are supplied to the burner via a pre-mix device; where the mixing is achieved by supplying at least one of the mixing agents in the form of a high speed jet [1]. In these cases, the specific mechanism of mixing is termed "entrainment" [4]. Typically, the gaseous fuel is supplied at a high velocity, with a high-low velocity interface generating shear and resulting in entrainment of the oxidiser [1].

A simplified cross-section of the pre-mixer considered for this work, is shown in Figure 1, where the dimensions of the mixer have been provided in terms of the gas jet nozzle's exit diameter, $D$. As illustrated by Figure 1 the pre-mixer consists of a convergent nozzle which creates a gaseous jet of fuel,

that passes into a chamber section which contains a further constriction (or throat), that provides an additional draw due to the drop in pressure caused by the "venturi" effect [5]. Subsequently, the velocity of the jet is more effectively increased, producing a greater pressure draw for the ambient air into the mixer's venturi chamber. An "adjuster plate" is incorporated into the design which can be moved to obstruct the quantity of air drawn through into the chamber. Generally, literature reports that an entrainment pre-mixer's operation is affected by several specifications, including: the venturi throat area; throat position; and, gas inlet location [5].

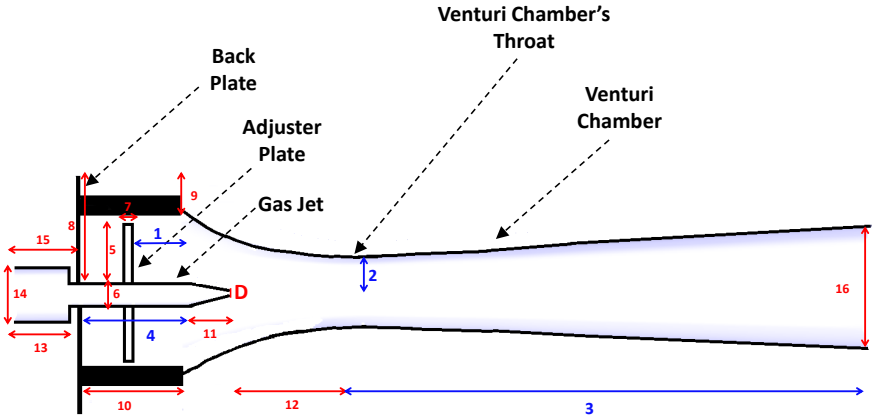


Dimensions in terms of gas jet nozzle's exit diameter, D mm :

| | | | | | | | |
|---|---|---|---|---|---|---|---|
| 1 | 11.2 | 5 | 16.68 | 9 | 8.72 | 13 | 13.53 |
| 2 | 9.12 | 6 | 6.47 | 10 | 23.53 | 14 | 13.53 |
| 3 | 130.59 | 7 | 1.77 | 11 | 10.81 | 15 | 18.82 |
| 4 | 25.29 | 8 | 25.41 | 12 | 29.41 | 16 | 30.59 |

**Fig. 1** A cross-section of the pre-mixer, with its relevant features labelled and dimensions provided in terms of the gas jet nozzle's exit diameter, $D$ mm; additionally, the dimensions 1 to 4 refer to the optimised design parameters

Previous work which has considered the simulation of pre-mix devices focussed on the assessment of the extent or quality of mixture between a gaseous fuel source and air supply. An approach of utilising the species transport model without reaction, in the commercial software package Fluent, has been implemented successfully to assess mixing between constituents. Yeap et al [6] clearly showed through CFD predictions that the incorrect location of the fuel injection point contributed to inhomogeneous mixing, with combustion efficiency dependant on the degree of homogeneous mixing of the air and fuel. They assessed the extent of mixing by plotting the averaged air-to-fuel ratio (AFR) value in radial planes at several axial locations downstream. Similarly,

Yusaf and Yusoff [7] adopted this approach and plotted the resulting natural gas concentrations in the radial and axial directions, to show the changes in concentration due to mixing. Additionally, measures such as standard deviation ($\sigma$) can be used as a post processing step to assess the extent of mixing between species in a CFD simulation. In work by Singh [8], this type of approach was implemented, with "an intensity of segregation as a measure of mixing defined as the second-moment variance of concentration distribution".

Simulation of turbulence is a critical part of modelling a device which premixes gases for combustion; when the turbulence energy dissipation rate ($\epsilon$) increases, turbulence and shear between the fuel and air streams increases resulting in a faster mix [4]. In the majority of work reviewed on simulation of pre-mixer type devices, the Standard $k$-$\epsilon$ turbulence model is utilised. Gorjibandby and Sangsereki [9] found that the Standard $k$-$\epsilon$ model provided the best balance between computational time and accuracy for a subsonic internal flow in a air-gas venturi mixer used for a bi-fuel diesel engine. Yusaf and Yusoff [7] employed the Standard $k$-$\epsilon$ model for a steady-state simulation of a 3D, eight hole, air-gas mixer, which provided realistic results for a well-bounded high Reynolds number flow.

Typically, the pre-mixers are available as COTS. This research work has considered such a device, with the intention of using a validated CFD simulation of the pre-mixer coupled with a Goal Driven Optimisation (GDO) process, to establish if the COTS device is optimised for its specific use. Subsequently in Section 3, a brief description of the experimental procedure implemented to attain measurements from an operational pre-mixer has been provided. These experimental results were then used in validating the CFD model, the implementation of which has been described in Section 4 and Section 5. Section 6 provides an overview of the optimisation techniques which were coupled with the CFD model to investigate the proficiency of the pre-mixer's operation. A summary of results from this work is provided in Section 7; with, conclusions regarding the outcome of the investigation provided in Section 8. The following Section 2, provides further background to that provided in Section 1 regarding the pre-mixer's operation, focusing upon the aspects of its performance that must be optimised and the parameters which affect these.

## 2 Defining objectives for optimisation

The first critical step in being able to optimise the pre-mixer is the identification of the outputs or measures which can be used to assess its optimality of operation to define an objective function [11]. Considering that the pre-mixer must provide a burner with the correct ratio of air and gaseous fuel that is thoroughly mixed to ensure efficient combustion, two clear objectives can be defined for the pre-mixer's operation:

1. Achieving the correct Air-to-Fuel Ratio (AFR) for combustion, with the required percentage of excess air.

2. The complete mixing of the air and fuel prior to entry to the combustion chamber.

The second step requires establishing what measurements can be used to quantify these objectives:

1. AFR for optimised combustion may be assessed as a scalar quantity; specifically, for the pre-mixer investigated for this research, 30% excess air was required for combustion. Consider a natural gas supply to the pre-mixer of the composition as summarised in Table 1. Utilising these data, the stoichiometric AFR calculated using mass is found to be 16. Consequently, when considering the required 30% excess air for efficient combustion, the mass-based AFR required is approximately, $(16 \times 1.3) = 21$. The attainment of this value will indicate that the required mixture of natural gas and air has been achieved.
2. Mixedness may be assessed based on the assumption that the percentage mass value of the air or natural gas constituents reach a constant value across the pre-mixer outlet's cross-section. This can be measured using the standard deviation ($\sigma$) value of the mass concentration of the air or natural gas constituents; where, a $\sigma$ value of zero would imply that a constant, completely mixed state has been achieved.

**Table 1** Natural Gas composition as supplied by Company

| Constituent | Percentage Composition (%) |
|---|---|
| Methane ($CH_4$) | 89.44 |
| Ethane ($C_2H_6$) | 5.43 |
| Propane ($C_3H_8$) | 1.40 |
| Butane ($C_4H_{10}$) | 0.40 |
| Nitrogen ($N_2$) | 1.95 |
| Carbon Dioxide ($CO_2$) | 1.35 |

Subsequently, the objective function can be written as:

$$f(\mathbf{x}) = w_1\sigma_A + w_2\sigma_M + w_3(21 - AFR_m) \tag{1}$$

Where, $\sigma_A$ is the standard deviation of the mass concentration of air across the pre-mixer's outlet; $\sigma_M$ is the standard deviation of the mass concentration of methane across the pre-mixer's outlet; and, $AFR_m$ is the AFR value calculated using the mass of air drawn in by the mixer and the mass of fuel gas supplied. The values $w_1$, $w_2$, and $w_3$, are constant values or weights which can be applied to the objectives and used to tune the objective function to find the desired balance for the multi-objective problem. Considering Equation 1, an excess air content greater than 30% would lead to negative $f(\mathbf{x})$; whilst, an excess air content less than 30% would result in positive $f(\mathbf{x})$. Therefore,

for an optimised 30% excess air content that was well mixed $f(\mathbf{x})$ must equal zero.

The objective function, will in turn, be dependent upon design parameters. Four dimensions of the pre-mixer were identified as being critical to its effectiveness. These design parameters are labelled (1 to 4) in Figure 1 and include: 1.) The position of the adjuster plate (DP1); 2.) the radius of the venturi chamber's throat (DP2); 3.) the length of the venturi chamber (DP3); and 4.) the extent which the fuel jet's nozzle extends into the venturi chamber (DP4).

However, prior to undertaking any simulation work for the optimisation process, it was necessary to acquire measurements regarding the pre-mixer's operation. The following Section 3 describes the experimental procedure implemented to attain such data.

## 3 Experimental procedure

In order to establish confidence in the CFD results and subsequent optimisation of the pre-mixer, experimental work was undertaken (using air only) to establish the effect of adjuster plate position on the flow's velocity at the pre-mixer's outlet. The adjuster plate was moved through several pre-marked locations. Air pressurised to $1.4 \times 10^5$ Pa was supplied to the gas jet inlet. Intrusive methods of velocity measurement were utilised, in the form of a vane anemometer, to take average velocity readings at the pre-mixer's outlet. Figure 2 illustrates the experimental set-up. At the measurement locations, flow disruptions such as shock waves were not expected; therefore, intrusive methods were deemed acceptable and the timeliest approach to utilise. The experimental data acquired were used for validation of a CFD simulation of the pre-mixer, with the CFD approach implemented described in the following Section 4.

**Fig. 2** The experimental set-up utilising the vane anemometer to measure the average velocity at the pre-mixer's outlet

## 4 The CFD model

The CFD for this study was undertaken using the Fluent v14.5 software [12], with the 3D problem solved making use of its axi-symmetry to reduce computational expense. Fluent utilises a cell-centred finite volume method. For this work, the governing equations were discretised using a second-order upwind scheme, using the SIMPLE algorithm to couple the momentum and pressure equations when using the pressure-based solver [13]. An assessment of turbulence models was made, supported by literature [9, 7] and from comparing the simulated average velocity values at the pre-mixer's outlet with those measured experimentally. The turbulence models considered included the Standard $k$-$\epsilon$, the Realisable $k$-$\epsilon$, the Modified $k$-$\epsilon$, and the $k$-$\omega$. Table 2 provides a summary of the average velocity values and the percentage differences with the experimental value, with the adjuster plate at a distance of $7.5D$ from the venturi chamber's inlet. Consequently, it was established that the Standard $k$-$\epsilon$ model was the most appropriate for this particular simulation [14, 15].

For the simulation, pressure to the gas jet was set at $1.4 \times 10^5$ Pa, the same as that used experimentally; whilst, the pressure at the air inlet and at the mixer's outlet was set as atmospheric.

**Table 2** A comparison of average velocity at the pre-mixer's outlet with the adjuster plate at a distance of 7.5D from the venturi chamber's inlet

| Turbulence Model | Area-av. Vel. (m/s) | Diff. frm experimental value (%) |
|---|---|---|
| Standard $k$-$\epsilon$ | 15.7 | 12.7 |
| Realisable $k$-$\epsilon$ | 14.7 | 18.3 |
| Modified $k$-$\epsilon$ | 12.8 | 28.8 |
| $k$-$\omega$ | 13.4 | 25.5 |

## 5 The species model

When simulating the mix between the natural gas and air, the percentage mass of each constituent was required; with the composition of natural gas as summarised previously in Table 1. To achieve this a species transport model was used, which applies a conservation equation to each of the different species. A local mass fraction for each species $m_i$ is predicted through the solution of a convection-diffusion equation for the $i^{th}$ species. This conservation equation takes the following general form:

$$\frac{\partial}{\partial t}(\rho m_i) + \frac{\partial}{\partial x_i}(\rho u_i m_i) = -\frac{\partial}{\partial x_i} J_i + G_i + S_i \tag{2}$$

where, $G_i$ is the net rate of production of species $i$ by chemical reaction; which is discounted if there is no reaction, as for this work. $S_i$ is the rate of creation by addition from the dispersed phase and $J_i$ is the diffusion flux of the species $i$, modelled using *"Fick's law"* [12,16]. Equation 2 is solved for $(N-1)$ species; where, $N$ is the total number of fluid phase chemical species present in the system.

Utilising the local mass fractions, the extent of mixing for various species can be determined; an essential measurement to acquire for the optimisation of the pre-mixer, with the optimisation processes considered and utilised described in the following Section 6.

## 6 The optimisation process

The optimisation of the pre-mixer was undertaken using Design Exploration (DE) v14.5 [17]. This allowed CFD simulations to be fed directly into the optimisation tool, creating a closed-loop from geometry, through simulation, to optimised design. The DE software works on the premise of Goal Driven Optimisation (GDO), which utilises a constrained, multi-objective optimisation technique, allowing the best possible designs to be identified from a sample set, derived from goals or targets set for the objectives [17]. A multi-objective formulation is a more realistic model for complex, real-world, engineering optimisation problems [18]. When considering these types of problems, typically, the objectives considered will conflict with each other. Therefore, considering

the optimisation of one objective at a time, in isolation, will not generate an optimum solution for the multi-objective problem under consideration [19]. The Ansys software utilises an approach where a "Pareto" optimal solution is achieved for the multi-objective optimisation [17], which comprises a set of optimal solutions that are non-dominated with respect to each other [18]. A Pareto optimal solution cannot be improved without worsening at least one other objective [19,14].

The overall optimisation process comprised three steps: the initial sampling step; followed by appropriate interpolation; and finally, using the data from the preceding two steps, the actual optimisation. For each of the steps, a range of options were considered to allow the most suitable and robust process to be implemented. Two sampling approaches were considered: a Design of Experiments (DoE)- Central Composite Design [20,21,14]; and, Optimal Space Filling (OSF) [22,21]. By considering these two approaches, data from both a regimented factorial approach, where the design space is split into repeated patterns and an approach where the design space is filled in a completely randomised manner were obtained. The DoE approach lends itself to the accurate interpolation of a second-order response surface [23]; whilst, OSF is better suited to more complex interpolation methods, e.g. Kriging [17,14].

Simulation optimisation requires that an objective function $f(\mathbf{x})$ is approximated based on the outputs of simulation runs [11]. These simulation runs will be undertaken for the parameter values chosen from the sampling method utilised, to obtain the most information about the constrained design space. Using the outputs from the selected simulation runs, a "meta-model" can be constructed to describe the relationship between $\mathbf{x_n}$ and $f(\mathbf{x_n})$ [24]. Therefore, reducing the CPU cost associated with running multiple simulations, as only the $n$ sample points are required.

Typically, the construction of the meta-model requires the implementation of some form of interpolation technique. Three different response surface types or meta-models were considered: a full second-order polynomial [17,25]; Kriging [26,17,11]; and a Neural Network (using three cells) [27,10,28].

The final step of the process utilises the sampling and interpolation data with the optimisation algorithm. The Multi-Objective Genetic Algorithm (MOGA) available within DE utilises the Non-dominated Sorted Genetic Algorithm-II (NSGA-II) [19,17]; described by Khalkhali et al [29] as "one of the most powerful evolutionary algorithms for solving multi-objective optimisation problems". The NSGA-II, by using a population of solutions can find multiple "Pareto-optimal" solutions in one single optimisation run. Using the response surface, an initial population for the NSGA-II of 10,000 was created; using this large initial population, means that its more likely the input parameter space that contains the best solutions will be identified [17]. However, utilising such a large initial population does come with an associated computational expense. The number of samples per iteration was set at 250, along with a Pareto percentage of 70% [17].

Additionally, within the DE software a Decision Support Process (DSP) can be applied to the Pareto fronts generated by the MOGA. This allows

a balance to be found between the multiple objectives by the application of weighting factors, which aid in fulfilment of the optimisation criterion [17]. On investigating the best implementation of the DSP in attaining the previously defined objective function, it was established that the attainment of $\sigma$ values of zero should be set with a low weighting, i.e. $w_1$ and $w_2$ of 0.33; whilst, achieving the correct $AFR_m$ value of 21 should be set at a high weighting, i.e. $w_3$ of 1.00 [14].

The optimisation process was initially undertaken considering only design parameters DP1 and DP2, then with DP3 and finally with DP4 included. This approach was undertaken to clearly establish the effect of the four parameters on the pre-mixer's performance.

For comparative purposes and to provide further confidence in the sampling results, an alternative optimisation algorithm was considered in the form of the Nelder Mead Method [30]. Utilising the same OSF sampling data, along with a Kriging interpolation, the optimisation was undertaken for the four design parameters DP1 to DP4, only. Nelder Mead is an example of a deterministic technique which uses the concept of simplices to represent the agents in the search space [30]. In this paper an implementation available as part of the MATLAB optimisation toolbox has been utilised [32]. This algorithm takes a single starting point as its input, which has been taken at the centre of the design space; a weighted objective function as in Equation 1 was used, with the same $w_1$, $w_2$ and $w_3$ values as those quoted previously, this was interpolated separately.

The results from the simulation and optimisation work are provided in Section 7.

## 7 Results

The axi-symmetric CFD simulation domain was discretised into several structured meshes, each with elements focused in the region of the issuing jet and at the walls, as clearly illustrated in Figure 3. The boundary conditions of pressure inlet, pressure outlet and wall used for the model are also labelled in Figure 3.

### 7.1 Mesh sensitivity and convergence

A full convergence and mesh sensitivity study was undertaken, with the steady-state solution considered converged when the discharge from the pre-mixer's outlet was found to differ by no more that 1%. Mesh independence was achieved with a mesh size consisting of 46,000 elements, i.e. an element dimension of $\delta$; with meshes considered of the order: $0.25\delta$; $0.5\delta$; $\delta$; $2.0\delta$; and, $3.5\delta$. The mesh sensitivity results are summarised in Table 3. It should be noted, that $\delta$ equates to approximately $2.5D$.

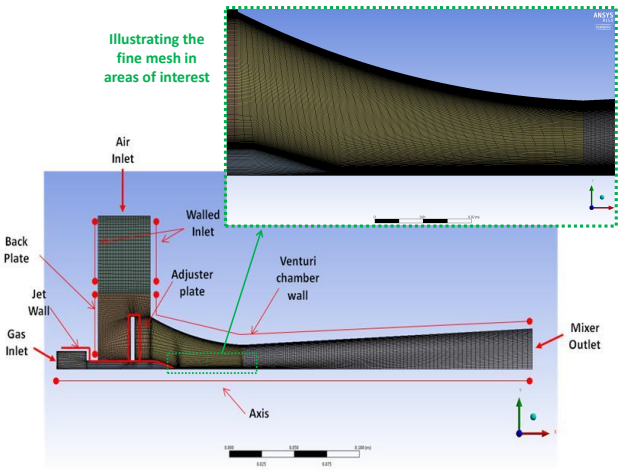


**Fig. 3** The mesh applied to the axi-symmetric geometry, showing the refinement in close-up at areas where more complex flow behaviour was anticipated. Additionally, the various boundary conditions are shown

**Table 3** Summary of the effect of mesh spacing on the discharge at the pre-mixer's outlet for the axi-symmetric CFD simulation

| Mesh element size (x $\delta$) | % diff. of discharge values compared with the finest mesh |
|---|---|
| 3.5 | 2.73 |
| 2.0 | 1.14 |
| 1.0 | 0.82 |
| 0.5 | 0.01 |
| 0.25 | 0.00 |

## 7.2 Validation of the CFD model

Figure 4 provides a comparison between the experimentally measured and simulated discharge at the pre-mixer's outlet; with varying adjuster plate location, when considering air as the only medium. It is evident that a similar trend is captured; where, pulling back the adjuster plate beyond a certain distance from the venturi chamber inlet, no longer has any effect on the quantity of air inspirated. The discharge velocity values levelled out to a maximum value of approximately 18 m/s (experimentally), and 16.5 m/s (simulated). It can be concluded that the simulation has accurately captured the fluid dynamics of the pre-mixer. The difference between the experimental and simulated results could potentially be attributed to a slight disruption of the flow due to the intrusive experimental measurement techniques employed.

Figure 5 shows the velocity and pressure contours from the simulation with the adjuster plate at a position of 7.06D mm from the venturi chamber's inlet.

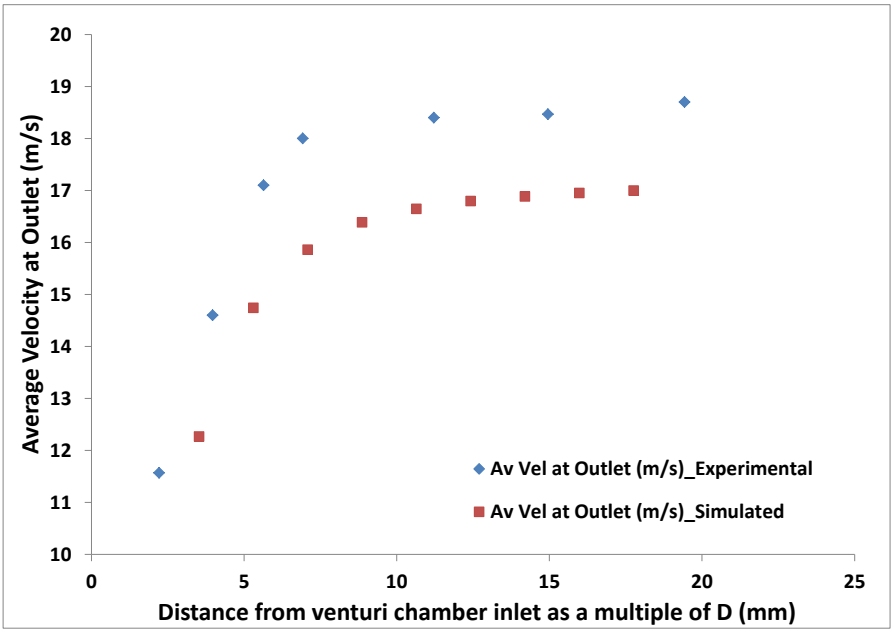


**Fig. 4** Experimental and CFD results showing the effect of adjuster plate position on velocity at the pre-mixer's outlet.

The negative pressure draw created at the venturi chamber throat and the subsequent effect this has on velocity is evident.

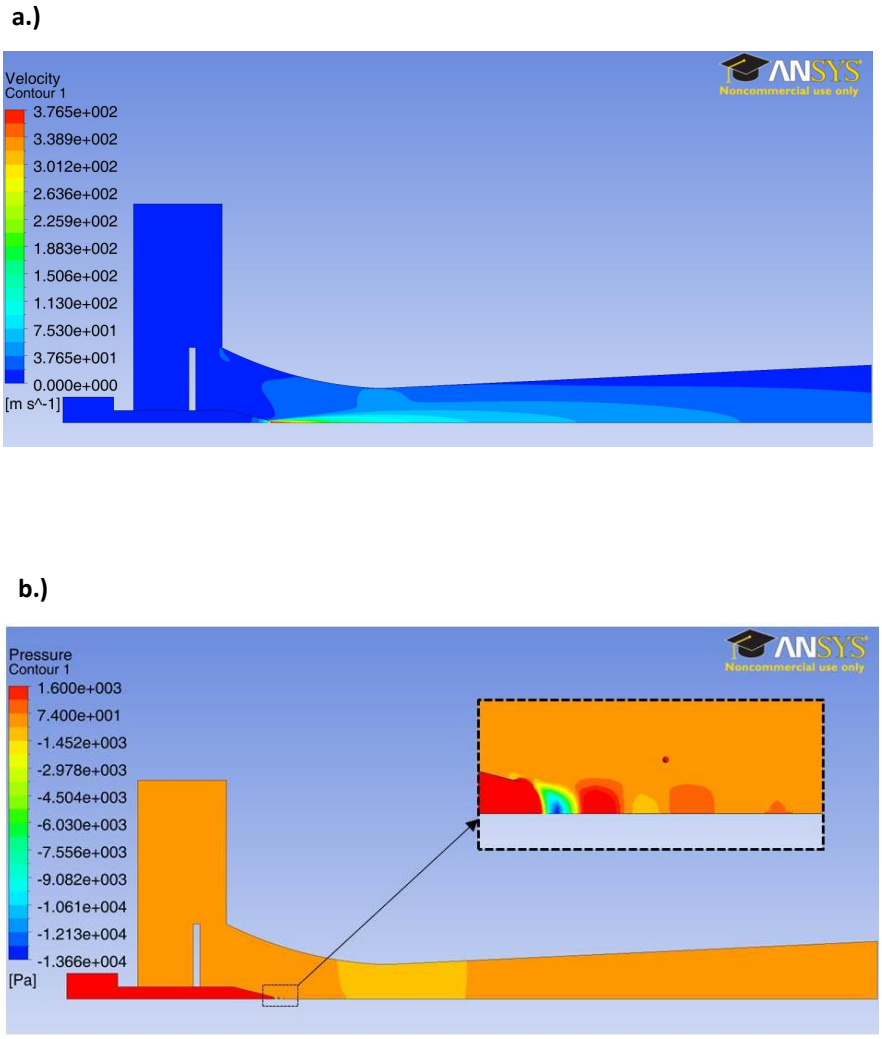


**Fig. 5** Using the Standard $k$-$\epsilon$ turbulence model taken from the axi-symmetric simulation of the pre-mixer showing a.) the velocity contour plot and b.) the pressure contour plot - within a specified pressure range.

Based on the validated axi-symmetric model which had only considered air as the working medium, further simulations were undertaken utilising the multi-species model, to simulate the mixing and interaction of air with natural gas in the pre-mixer. Figure 6 shows an example of the species contours generated for methane and air, when natural gas is supplied at the gas inlet and the adjuster plate is located at a position of 7.06D mm from the venturi chamber's inlet.

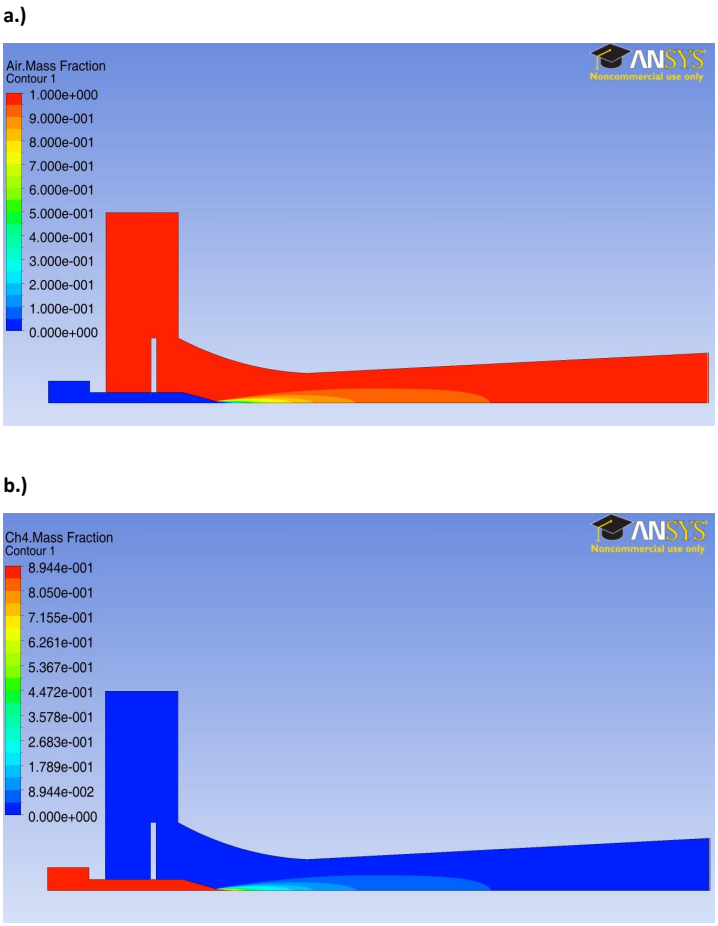


**Fig. 6** Species concentration contours for a.) air and b.) methane generated from the multi-species simulation using the Standard $k$-$\epsilon$ turbulence model, taken from the axi-symmetric simulation of the pre-mixer.

Utilising the output parameters from the CFD simulation, values were calculated at the pre-mixer's outlet for $\sigma_M$, $\sigma_A$ and $AFR_m$, these are summarised in Table 4.

**Table 4** Summary of the objective parameter values achieved from the multi-species, axi-symmetric CFD simulation of the initial pre-mixer's design, with the adjuster plate positioned 7.06D mm from the venturi chamber's inlet.

| Objective Parameter | Value from initial design's CFD simulation |
|---|---|
| Mass AFR | 20.957 |
| SD of Air | 6.00 e-05 |
| SD of Methane | 5.40 e-05 |

### 7.3 The identification of a suitable sampling and interpolation approach

Following validation of the CFD model, it was necessary to establish the most appropriate sampling and interpolation approach to be used for the pre-mixer's optimisation. Using a sample set generated from the DoE - Central Composite (Face Centred Enhanced) approach, it was possible to compare the Goodness of Fit (GoF) charts [17] for each interpolation approach.

The GoF chart presents a view of output parameter values predicted from the interpolation/response surface, versus values calculated from the CFD simulation (i.e. the sampling points). The closer the points fit a straight line, the better the prediction. In addition to using the sampling values, verification points were also included i.e. randomly generated design points; with these clearly identified in the GoF plots shown in Figure 7.

These verification points provided a further opportunity with which to assess the accuracy of the interpolation techniques; but, were particularly important in the assessment of the Kriging technique. The Kriging approach interpolates through all sampling points, which results in a GoF illustrating data which is exactly fitted to the straight line [25]. The inclusion of the verification points overcomes this issue, as their proximity to the straight line can be used to assess the actual predictive accuracy of the interpolation. It is evident from the plots, shown in Figure 7, that each of the interpolation approaches gives reasonably accurate predictions, with the exception of one of the verification points, for which each of the interpolation methods has struggled. It is potentially because this point lies in a region with little information from the sampling set, which has led to inaccuracies for the interpolation. However, as all three approaches have the same problem, this point has been discounted in assessing which interpolation approach is most appropriate.

a.)

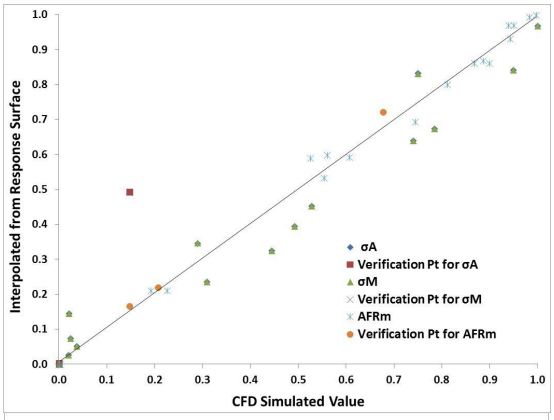


b.)

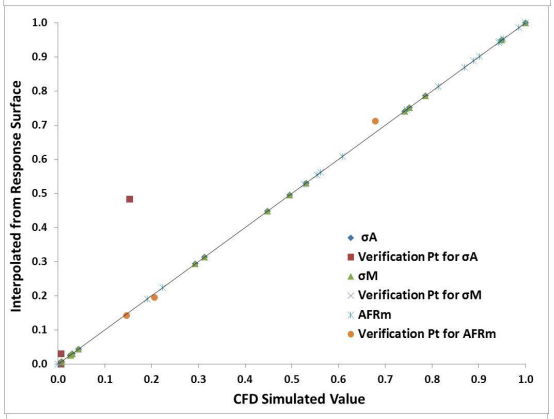


c.)

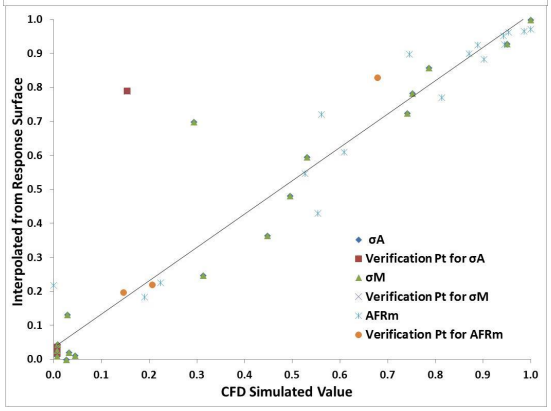


**Fig. 7** Goodness of Fit (GoF) charts providing an overview of output parameter values predicted from the interpolation surface, versus CFD simulated values for: a.) second-order response surface; b.) Kriging; and c.) Neural Network interpolation approaches. The closer the points fit a straight line, the better the prediction.

An in-depth analysis of the optimised results [14], established that OSF, implemented with a maximum number of 50 iterations to establish the sample set [17], when used with a Kriging interpolation provided the most robust optimisation approach for the pre-mixer considered. A summary of these results is provided in Table 5. The analysis was based on an approach using the DoE sampling method and comparing the NSGA-II optimised results after considering the three interpolation methods. From Table 5 it can be seen that the second-order response surface failed to minimise the $\sigma$ values measuring the extent of mixing, whilst achieving an $AFR_m$ value of 21 [14]. The Neural Network (NN) approach effectively minimised the $\sigma$ values, improving mixing by approximately 15% but at the expense of attaining an $AFR_m$ value of 21 [14]. The Kriging approach performed better, achieving an improvement in mixing of approximately 37%, but with an AFR that was still 5% below 21 [14]. Consequently, both the DoE and OSF sampling approaches were compared using the Kriging interpolation method. From Table 5, it can be seen that the latter provided more balanced results with regards to the requirements of the optimisation; achieving an improvement in mixing of approximately 16% and an AFR value only 2% from the required 21. Typically, OSF is a more efficient sampling scheme when implementing complex meta-modelling techniques like Kriging. Subsequently, these sampling and interpolation methods were implemented for a full optimisation based study of the pre-mixer.

**Table 5** A comparison of results from various sampling and interpolation models

| Sampling | Interpolation | $\sigma_A$ (e-05) | $\sigma_M$ (e-05) | % ↑ mixing | $AFR_m$ | % dev. frm 21 |
|---|---|---|---|---|---|---|
| DoE | $2^{nd}$ order | 6.10 | 5.45 | - | 21.146 | 0.7 |
| DoE | Kriging | 3.76 | 3.36 | 37 | 19.79 | 5.8 |
| DoE | NN | 2.86 | 2.56 | 52 | 18.96 | 9.7 |
| OSF | Kriging | 5.08 | 4.54 | 15 | 20.579 | 2.0 |

## 7.4 Optimisation results

Generally, on reviewing the results from the NSGA-II optimisation process, it became evident that there was conflict between achieving an $AFR_m$ value of 21 and reducing the $\sigma$ values to as close to zero as possible. That was, the further the $AFR_m$ value deviates from 21, the greater the reduction in $\sigma$ values as compared to the initial design's. The results for two (DP1 and DP2), three (DP1 to DP3), and four (DP1 to DP4) parameters, are summarised in Table 6, where the best result from the Pareto set of three optimised results has been presented as multiples of the gas jet nozzle's diameter $D$, for each case. A bracketed percentage value is provided alongside the parameter dimension which indicates the change required in the pre-mixer's optimised design

parameters as compared to the initial design. Considering the $\sigma$ values, the percentage difference bracketed alongside represents a decrease in the $\sigma$ value from the initial design (i.e. an improvement in mixing). For the $AFR_m$ values, a percentage difference from the required value of 21 is provided along with $\uparrow$, indicating the $AFR_m$ value is above 21, or $\downarrow$ if below.

**Table 6** The "best" optimised results using the NSGA-II algorithm; including the design parameters initial and optimised in terms of the gas jet nozzle's exit diameter, D; and, the percentage differences in design parameters and objective outputs as compared to the initial design.

| | Initial Design | 2 Parameters | 3 Parameters | 4 Parameters |
|---|---|---|---|---|
| DP1 (mm) | 14.7 | 10.18 (44%) | 8.53 (21%) | 8.88 (26%) |
| DP2 (mm) | 9.12 | 9.47 (4%) | 9.47 (4%) | 9.47 (4%) |
| DP3 (mm) | 130.59 | 130.59 (0%) | 143.41 (10%) | 134.88D (3%) |
| DP4 (mm) | 1.76 | 1.76 (0%) | 1.76 (0%) | 2.76 (57%) |
| $\sigma_A$ (e-05) | 6.00 | 5.08 (15%) | 4.19 (30%) | 4.20 (30%) |
| $\sigma_M$ (e-05) | 5.40 | 4.54 (16%) | 3.74 (31%) | 3.76 (30%) |
| $AFR_m$ | 20.96 | 20.58 (2% $\downarrow$) | 21.29 (1% $\uparrow$) | 20.64 (2% $\downarrow$) |

Results from implementing the Nelder Mead Method for the four design parameters is presented in Table 7, which provides a comparison with the initial design and NSGA-II optimisation.

**Table 7** Results from the Nelder Mead Method and the NSGA-II algorithm for design parameters DP1 to DP4; including the design parameters initial and optimised in terms of the gas jet nozzle's exit diameter, D; and, the percentage differences in design parameters and objective outputs as compared to the initial design.

| | Initial Design | NSGA-II | Nelder Mead |
|---|---|---|---|
| DP1 (mm) | 14.7 | 8.88 (26%) | 6.45 (56%) |
| DP2 (mm) | 9.12 | 9.47 (4%) | 9.23 (1%) |
| DP3 (mm) | 130.59 | 134.88D (3%) | 146.47 (13%) |
| DP4 (mm) | 1.76 | 2.76 (57%) | 2.34 (33%) |
| $\sigma_A$ (e-05) | 6.00 | 4.20 (30%) | 3.975 (33%) |
| $\sigma_M$ (e-05) | 5.40 | 3.76 (30%) | 3.56 (34%) |
| $AFR_m$ | 20.96 | 20.64 (2% $\downarrow$) | 21.58 (3% $\uparrow$) |

Considering the four parameter optimisation; Figure 8 provides the global sensitivities of the output objectives with respect to the input parameters. It is clearly evident from this chart that the radius of the venturi chamber's throat (DP2) is the parameter the objective function measures (i.e. $\sigma$ and $AFR_m$) are most effected by; the length that the fuel jet extends into the venturi chamber (DP4) has limited, if any effect; whilst, both the position of the adjuster plate (DP1) and the length of the venturi chamber (DP3) have a comparatively moderate effect.

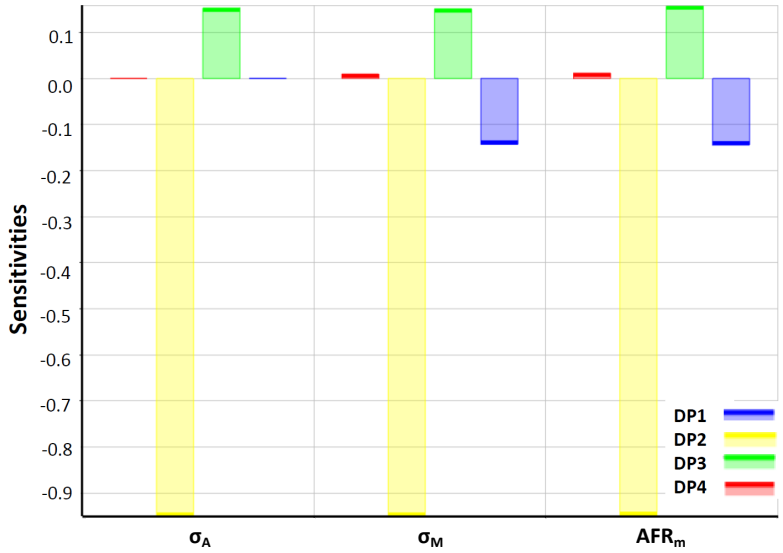


**Fig. 8** The global sensitivities of the defined objective parameters with respect to the four design parameters (DP1 to DP4) considered for the optimisation of the pre-mixer

The outcome of the extensive optimisation based investigation is that the current design of the COTS pre-mixer can with slight modifications of its design, provide improvement in mixing quality. Both the NSGA-II and Nelder Mead algorithms verified this to be around 30%, whilst maintaining the AFR within 2-3% of the required value. Overall conclusions regarding the optimisation work are provided in the final Section 8.

## 8 Conclusions

In order to carry out a thorough investigation into the optimality of the COTS venturi-type pre-mixer, it was critical to establish clear objectives and measures of these with which to undertake the GDO process. These objectives can be extracted from a clear understanding of what the equipment's role is;

particularly, specific requirements of the combustion process/equipment that it is supplying.

By utilising CFD in conjunction with the optimisation process it was possible to achieve an in-depth understanding of the pre-mixer's operation. It was observed that when considering only three design parameters (i.e. discounting DP4), the best results were achieved in the sense of fulfilling the optimisation requirements; this is potentially attributable to the fact that as identified by the global sensitivity study, DP4 was the least consequential design parameter with regards pre-mixer performance.

Considering the objective function and its requirements of efficient mixing alongside the maintenance of a defined mix ratio, it was established from the optimisation results that there is a trade-off between these two requirements. That is, the greater the extent of minimisation of the $\sigma$ values (i.e. mixing), the further the $AFR_m$ value moves from (typically below) the required value (i.e. mix ratio).

A comparison of sampling and interpolation techniques within the Ansys Design Exploration (DE) software, established that OSF with a Kriging interpolation approach were most applicable to this problem.

From the optimisation it was established, by both the NSGA-II and Nelder Mead algorithms, that an approximate 30 % improvement in the extent of mixing could be achieved with modification to the COTS design. With this information, the Company utilising the pre-mixer can decide whether the quantifiable gain in performance is worth the cost of modifying the current COTS design.

Further work on this topic is ongoing to assess the viability of using an alternative evolutionary type algorithm for the optimisation process. Additionally, there is scope to consider more radical or novel pre-mixer designs and their usability for specific industrial combustion processes.

**Acknowledgements** The authors would like to acknowledge the financial support of EPSRC, the Welsh Government and the European Regional Development Fund through ASTUTE project (WEFO project ID 80380) and the ASTUTE 2020 operation, currently funded by the College of Engineering, Swansea University, in enabling the research upon which this paper is based.

## References

## References

1. J. Baukal, E. Charles, *The John Zink Hamworthy Combustion Handbook: Volume 1-Fundamentals* (CRC Press, 2012)
2. W. Bussman, C. Baukal, Energy **34**(10), 1624 (2009)
3. M.E. Porter, C. Van der Linde, The journal of economic perspectives pp. 97–118 (1995)
4. J. Zhang, Micro injection fuel/air premixer/combustion. Ph.D. thesis, Faculty of the Louisiana State University and Agricultural and Mechanical College (2007)
5. D. Danardono, K. Kim, S. Lee, J. Lee, Journal of mechanical science and technology **25**(9), 2285 (2011)

6. B. Yeap, A. Mustafa, Z. Yaacob, in *Proceedings of The 15th Symposium of Malaysian Chemical Engineers SOMChE 2001* (2001)
7. T. Yusaf, M. Yusoff, in *Proceedings of the International Conference and Exhibition and Natural Gas Vehicles* (IANGV International Association of Natural Gas Vehicles, 2000)
8. M. Singh, Design, analysis, and optimization of distributive mixing: with applications to micro and industrial flow devices. Ph.D. thesis, Technische Universiteit Eindhoven (2008)
9. M. Gorjibandpy, M. Sangsereki, World Academy of Science, Engineering and Technology **71** (2010)
10. P. Papalambros, D. Wilde, *Principles of optimal design: modeling and computation* (Cambridge university press, 2000)
11. W. Hare, J. Nutini, S. Tesfamariam, Advances in Engineering Software **59**, 19 (2013)
12. Ansys. Fluent theory guide v14.0. Online, page visited January 2014 (2013). URL `http://www.ansys.com`
13. H. Versteeg, W. Malalasekera, *An introduction to computational fluid dynamics: the finite volume method* (Pearson Education, 2007)
14. J. Thompson, The development of simulation procedures for industrial mixing processes. Ph.D. thesis, Swansea University (2015)
15. J. Thompson, O. Hassan, D. Carswell, N. Lavery, S. Rolland, J. Sienz, in *Proceedings of the 22nd UK Conference of the Association for Computational Mechanics in Engineering* (ACME, 2014)
16. R. Kamali, A. Binesh, International Communications in Heat and Mass Transfer **36**(9), 978 (2009)
17. Ansys. Fluent user guide v14.0. Online, page visited January 2014 (2013). URL `http://www.ansys.com`
18. A. Konak, D. Coit, A. Smith, Reliability Engineering & System Safety **91**(9), 992 (2006)
19. R. Evins, Renewable and Sustainable Energy Reviews **22**, 230 (2013)
20. S. Ferreira, R. Bruns, H. Ferreira, G. Matos, J. David, G. Brandao, E. da Silva, L. Portugal, P. Dos Reis, A. Souza, et al., Analytica chimica acta **597**(2), 179 (2007)
21. L. Pronzato, W. Müller, Statistics and Computing **22**(3), 681 (2012)
22. R. Jin, W. Chen, A. Sudjianto, Journal of Statistical Planning and Inference **134**(1), 268 (2005)
23. 
24. L. Wang, L. Shi, Acta Automatica Sinica **39**(11), 1957 (2013)
25. L. Rios, N. Sahinidis, Journal of Global Optimization **56**(3), 1247 (2013)
26. T. Simpson, T. Mauery, J. Korte, F. Mistree, AIAA journal **39**(12), 2233 (2001)
27. M. Anjum, I. Tasadduq, K. Al-Sultan, European Journal of Operational Research **101**(1), 65 (1997)
28. A. Zaabab, Q. Zhang, M. Nakhla, Microwave Theory and Techniques, IEEE Transactions on **43**(6), 1349 (1995)
29. A. Khalkhali, M. Mostafapour, S.M. Tabatabaie, B. Ansari, Structural and Multidisciplinary Optimization pp. 1–17 (2016)
30. J.A. Nelder, R. Mead, The Computer Journal **7**(4), 308 (1965)
31. J.C. Lagarias, J.A. Reeds, M.H. Wright, P.E. Wright, SIAM Journal of Optimization **9**, 112 (1998)
32. mathworks. fminsearch. Online, page visited October 2015 (2015). URL `http://uk.mathworks.com/help/matlab/ref/fminsearch.html?refresh=true`